ADVANCED MATERIALS TECHNOLOGIES
www.advmattechnol.de



# All Paper-Based, Multilayered, Inkjet-Printed Tactile Sensor in Wide Pressure Detection Range with High Sensitivity

*Taehoon Lee, Yunsung Kang, Kwanhun Kim, Sangjun Sim, Kyubin Bae, Yeunjun Kwak, Wonkeun Park, Minhyeong Kim, and Jongbaeg Kim**

**Paper has attracted considerable interest as a promising pressure-sensing element owing to its foldability/bendability and deformability due to its high porosity. However, paper-based tactile sensors reported hitherto cannot achieve high sensitivity and a wide sensing range simultaneously. In this study, a resistive tactile sensor using carbon nanotube- and silver nanoparticle-printed mulberry paper as a pressure-sensing element and electrodes, respectively, is developed. The rough surface and high inner porosity of mulberry paper induce a significant change in the contact area when a multilayer-stacked structure is used, resulting in increased sensitivity to pressure. Moreover, the enhanced mechanical robustness of mulberry paper originating from the highly bonded network of long and thick fibers affords a wide pressure-sensing range. The sensor exhibits a high sensitivity exceeding 1 kPa$^{-1}$ in an applied pressure range of 0.05–900 kPa; this achievement has not been reported among paper-based tactile sensors. Furthermore, the sensor exhibits a fast response/relaxation time, low detection limit, high resolution, high durability, and high flexibility. The advantages of the sensor afford several applications, including a crosstalk-free pressure sensor array, a three-axis pressure sensor, and wearable devices for measuring signals from a user.**

## 1. Introduction

Paper, which comprises many cellulose fibers resulting in a porous network structure, has garnered significant interest as a building material in flexible electronics because it is thin, low in cost, lightweight, renewable, biocompatible/biodegradable, and foldable/bendable.[1] In addition, various manufacturing techniques, including dip coating, direct writing, inkjet printing, screen printing, and gravure printing, can be easily integrated with paper, thereby enabling the mass production of a device at a low cost. This integration possibility has led to the rapid development of paper-based electronics. For instance, flexible electrodes,[2–4] light-emitting diodes,[5] thin-film transistors,[6] gas sensors,[7] energy harvesters,[8] ion detectors,[9] and supercapacitors[10] that apply the aforementioned properties of paper have been proposed and experimentally verified. Among various applications, paper-based tactile sensors that detect applied pressure have also garnered significant attention,[11–26] regardless of their sensing principles based on changes in piezoresistivity, capacitance, and contact resistance. This is because paper can be utilized as a pressure-sensing structure owing to its high porosity and deformability. One of the paper-based tactile sensors reported showed a superior sensitivity of 1911.4 kPa$^{-1}$; however, it was limited to an extremely narrow range of applied pressure below 0.5 kPa.[24] Moreover, most of the studies mentioned above indicated a limited pressure-sensing range with linearity. Poor linearity implies that the tactile sensor should be calibrated under various pressures. The narrow pressure-sensing range renders it challenging to integrate a tactile sensor with applications requiring a wide pressure-sensing range. In addition, commercial paper exhibited vulnerability to acidic or organic chemicals,[27] which limited its development using various materials and its usage in diverse environments.

To overcome these limitations, mulberry paper has emerged as a promising alternative for use in paper-based electronics. It has been reported to possess a higher amount of holocellulose, i.e., a combination of cellulose and hemicellulose, than commercial paper. This high holocellulose content affords enhanced hydrophilicity[28,29] and induces the conformal formation of nanomaterials diluted in water when they are coated onto the fibers of mulberry paper. This is advantageous for resistive tactile sensors because it induces a stable and repeatable change in the contact area. Meanwhile, abundant —OH functional groups on the surface of holocellulose provide strong hydrogen bonding between fibers in the network structure of mulberry paper.[27] In addition, the fiber length and diameter of mulberry paper are longer and thicker than those of commercial paper.[30] This enhances the mechanical robustness of mulberry paper, reflected in its foldability and bendability. Moreover, mulberry paper has been reported to be highly resistant to chemicals because of its neutral pH value.[31] This prevents it from being affected by oxidation or acidolysis. In recent years, various electronic devices using mechanically robust and chemically

T. Lee, Y. Kang, K. Kim, S. Sim, K. Bae, Y. Kwak, W. Park, M. Kim, J. Kim
School of Mechanical Engineering
Yonsei University
50 Yonsei-ro, Seodaemun-gu, Seoul 03722, Republic of Korea
E-mail: kimjb@yonsei.ac.kr

The ORCID identification number(s) for the author(s) of this article can be found under https://doi.org/10.1002/admt.202100428.

DOI: 10.1002/admt.202100428

 

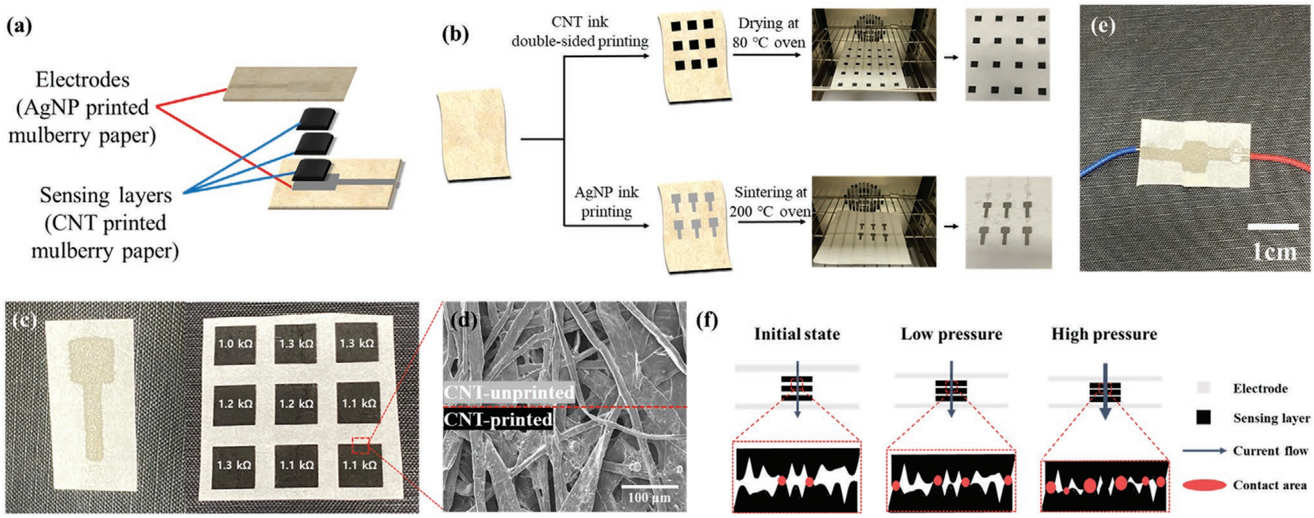


**Figure 1.** a) Schematic illustration of proposed tactile sensor using inkjet-printed mulberry paper. b) Preparation process of inkjet-printed mulberry paper. CNTs diluted in water were printed on both sides of mulberry paper using a commercial inkjet printer, followed by drying in an oven. AgNPs diluted in triethylene glycol monomethyl ether were printed on mulberry paper and subsequently sintered in an oven. c) Optical images of AgNP- and CNT-printed mulberry paper. Measured resistance of printed AgNP electrode was ≈40 Ω. Average resistance of CNT-printed mulberry paper was 1.18 kΩ with very low deviation (≈10.3%). d) SEM image at interface of CNT-printed and -unprinted mulberry paper. As shown clearly, CNTs were coated on mulberry paper without significant alteration on its fiber structure. e) Optical image of fabricated tactile sensor. f) Pressure-sensing mechanism of tactile sensor.

resistant mulberry paper have been introduced, such as supercapacitors,[30] flexible electrodes,[32] electromagnetic interference shielding materials,[33] and strain sensors.[34] However, to the best of our knowledge, a tactile sensor utilizing mulberry paper has not yet been reported.

In this study, a resistive tactile sensor based on the change in the contact area between electrical conductors is presented using stacked mulberry paper printed with carbon nanotubes (CNTs) as a pressure-sensing element. Inkjet printing is performed by covering the CNTs on both sides of mulberry paper. This technique affords the uniform formation of nanomaterials in small amounts, thereby affording a low cost of mass production. In addition, electrodes are formed on mulberry paper with inkjet-printed silver nanoparticles (AgNPs). Mulberry paper has a rough surface and a fiber-networked structure with high porosity; hence, it induces a significant change in the contact area between the sensing layer and electrodes when pressure is applied. Moreover, the stacked layers of CNT-coated mulberry paper allow an increased contact area and distributed stress on them, which is beneficial with regard to the sensitivity and sensing range of pressures. The fabricated sensor demonstrated sensitivity values of 6.67, 2.80, and 1.19 $kPa^{-1}$ to pressure ranging from 0.05 to 100 kPa, 100 to 300 kPa, and 300 to 900 kPa, respectively. The enhanced mechanical robustness of mulberry paper contributes to the wide sensing range, which has rarely been achieved in previous paper-based tactile sensors.[11–26] Furthermore, the sensor performance was compared with those of control devices using commercial printing and Kent paper, which revealed that our approach using mulberry paper is highly advantageous for obtaining high sensitivity and a wide sensing range. Finally, a pressure sensor array without crosstalk, a three-axis pressure sensor, and wearable applications were demonstrated using an all-paper tactile sensor.

## 2. Results and Discussion

### 2.1. Sensor Design and Fabrication

**Figure 1**a shows a schematic illustration of the proposed tactile sensor using inkjet-printed mulberry paper. For the formation of sensing layers, CNTs diluted in water were printed on both sides of the mulberry paper using a commercial inkjet printer, followed by drying at 80 °C in an oven for 10 min. Additionally, AgNPs diluted in triethylene glycol monomethyl ether were printed on mulberry paper and subsequently sintered at 200 °C in an oven for 20 min for use as electrodes in the tactile sensor. The preparation process for the nanomaterial-printed mulberry paper is shown in Figure 1b. In addition, the thickness of the mulberry paper was measured using a cross-sectional scanning electron microscope (SEM) image (Figure S1, Supporting Information), which was ≈200–300 µm. It clearly shows thicker fibers of mulberry paper than those of copy paper, thereby enhancing the porosity, which is advantageous for pressure sensing. Figure 1c shows optical images of the AgNP- and CNT-printed mulberry paper. The resistance measured from the top to the bottom of the printed AgNP electrode was ≈40 Ω. This is much lower than the average resistance of CNT-printed mulberry paper (1.18 kΩ), indicating that AgNP-printed mulberry paper can be utilized as electrodes. In addition, the resistivity of AgNP and CNT-printed mulberry paper was calculated as 16 and 472 kΩ m from the equation ($\rho = RAl^{-1}$), respectively, where $R$, $A$, and $l$ denote the resistance (40 Ω and 1.18 kΩ), area (1 $cm^2$), and length (250 µm), respectively. Meanwhile, the resistance measured for each CNT-printed area indicated a low deviation (≈10.3%). This reveals that our approach using inkjet printing to form nanomaterials on mulberry paper is highly advantageous for achieving uniformity of pressure-sensing elements. To confirm the infiltration of CNTs inside the mulberry paper, the cross-section of the mulberry paper was observed where they were printed on one side only (Figure S2a, Supporting Information). Infiltrated CNTs could be observed at ≈70% of the paper thickness from the printed side. Figure S2b,c in the Supporting Information shows the optical images of the front and back sides of the mulberry paper when CNTs were printed on one side only. Figure S2c in the Supporting Information shows that the CNTs were not exposed on the opposite side of the printed surface. In short, CNTs can infiltrate more than half of the thickness of the mulberry paper, and inkjet printing on both sides would be required to make an electrical connection through the paper thickness. Moreover, the above-mentioned resistance value of the CNT-printed mulberry paper was measured between the top and bottom electrodes after the CNTs were printed on both sides. This also indicates that a conductive CNT channel was formed through electrically insulating mulberry paper. Figure 1d shows a SEM image of the interface of the CNT-printed and -unprinted mulberry paper. As shown, the CNTs were coated on mulberry paper without any significant alteration in the fiber structure. Furthermore, enlarged SEM images of the CNT-printed mulberry paper were observed. As shown in Figure S3 in the Supporting Information, we confirmed that the CNT network was formed at three different positions of the fiber in the mulberry paper. This indicates a highly advantageous aspect of our approach using inkjet printing in that a CNT electrical channel should be formed along the fiber of the mulberry paper. The fabricated tactile sensor is shown in Figure 1e. As mentioned in the introduction, we used stacked multilayers of CNT-coated mulberry paper as the pressure-sensing element between the electrodes. This multilayer structure provides an additional contact area, inducing an increased sensitivity compared to that of a single layer, as well as a wide sensing range owing to the efficient stress distribution between layers.[35,36] The pressure-sensing mechanism of the tactile sensor is illustrated in Figure 1f. Mulberry paper is composed of interwoven fibers and has a rough surface.[37] Hence, only a few contact points are formed between layers of CNT-printed mulberry paper prior to applying pressures, resulting in a relatively high initial resistance (≈400 kΩ). As the applied pressure increased, the contact area between the rough surfaces of the CNT-printed mulberry paper increased. Consequently, this lowers the resistance of the sensor, i.e., increasing the current measured through the two AgNP-printed electrodes.

### 2.2. Pressure-Sensing Performance

**Figure 2** shows the overall pressure sensing characteristics of the sensor (see Figure S4 in the Supporting Information for details of the experimental setup). The current ($I$)–voltage ($V$) curves of the tactile sensor with three CNT-printed mulberry paper structures under various pressures from 1 to 500 kPa are presented in Figure 2a. The inset of Figure 2a shows the magnified $I$–$V$ curves of the tactile sensor with three CNT-printed mulberry paper structures under pressures of 1, 5, and 10 kPa. It clearly shows that the slope of the $I$–$V$ curves increased with pressure, indicating a decrease in resistance contributed by the increase in the contact area between layers. Figure 2b presents the relative change in the current of the sensors based on one-, two-, and three mulberry paper-layered structures at applied pressures from 1 to 900 kPa. Herein, the sensitivity of the sensor is defined as the relative change in current ($\Delta I$) divided by the initial current ($I_0$) and applied pressure. When calculating the sensitivity, we separated the range of applied pressures into three regions to satisfy that the coefficients of determination ($R^2$) were higher than 0.95. Hence, the sensitivity was calculated from 1 to 100 kPa ($R^2 \approx 0.962$), from 100 to 300 kPa ($R^2 \approx 0.9995$), and 300 to 900 kPa ($R^2 \approx 0.9885$) for presenting the values based on a somewhat linear range for comparison with previously reported studies. The measured sensitivities of the sensors based on one-, two-, and three-layered CNT-printed mulberry paper were 0.28, 3.61, and 6.67 $kPa^{-1}$ from 0 to 100 kPa, respectively, 0.17, 1.60, and 2.80 $kPa^{-1}$ from 100 to 300 kPa, respectively, and 0.07, 0.47, and 1.19 $kPa^{-1}$ from 300 to 900 kPa, respectively. As the number of CNT-printed layers increased, the effective contact area between them increased, thereby increasing the sensitivity of the sensor. These results imply that our approach using stacked CNT-printed mulberry paper as a pressure-sensing element is highly advantageous for achieving the high sensitivity of resistive tactile sensors. In addition, we observed three stacked layers of CNT-printed mulberry paper under compression at various pressure from a cross-sectional view, as shown in Figure S5 in the Supporting Information. Even though it is difficult to clearly show the change in contact area, the significant change in contact resistance indirectly reveals the physical contact area. Nonetheless, compression is clearly visible in the cross-sectional images as the pressure increases. This would induce an increase in the contact area, thereby leading to an increase in current through the sensor, which was also confirmed by the experimental results. The relative change in the current of the sensor based on the four mulberry paper-layered structures is presented in Figure S6 in the Supporting Information. An increase in the contact area of the sensor allows a slightly higher relative change in current in the low-pressure range than that of a three-layered structure. The increase in sensitivity as the layer increases is comparable to the tendency of the reported pressure sensor using a multilayer structure.[35] However, although we could observe a relative change in current with a precise sourcemeter, the high initial resistance of more than a megohm (1.43 MΩ) generated from the series connection of the four layers of resistors makes it difficult to integrate them for practical applications owing to the high level of noise.[36] Hence, we used a three-layered mulberry paper structure as the main structure of the sensor to show the overall pressure sensing characteristics. To verify the practicability of using mulberry paper as a structural material in the tactile sensor, we performed controlled experiments using printing and Kent papers, as shown in Figure 2c. CNTs were inkjet-printed on the copy and Kent papers under the same conditions, and the three-layered structure of each paper was used as the pressure-sensing element. However, the linear region of the two sensors was limited, and the sensitivities were much lower than those of the mulberry paper-based tactile sensor. This is attributed to the structural characteristics of mulberry paper. First, mulberry paper has an extremely rough surface compared to other papers; as such, they can be distinguished easily from

 

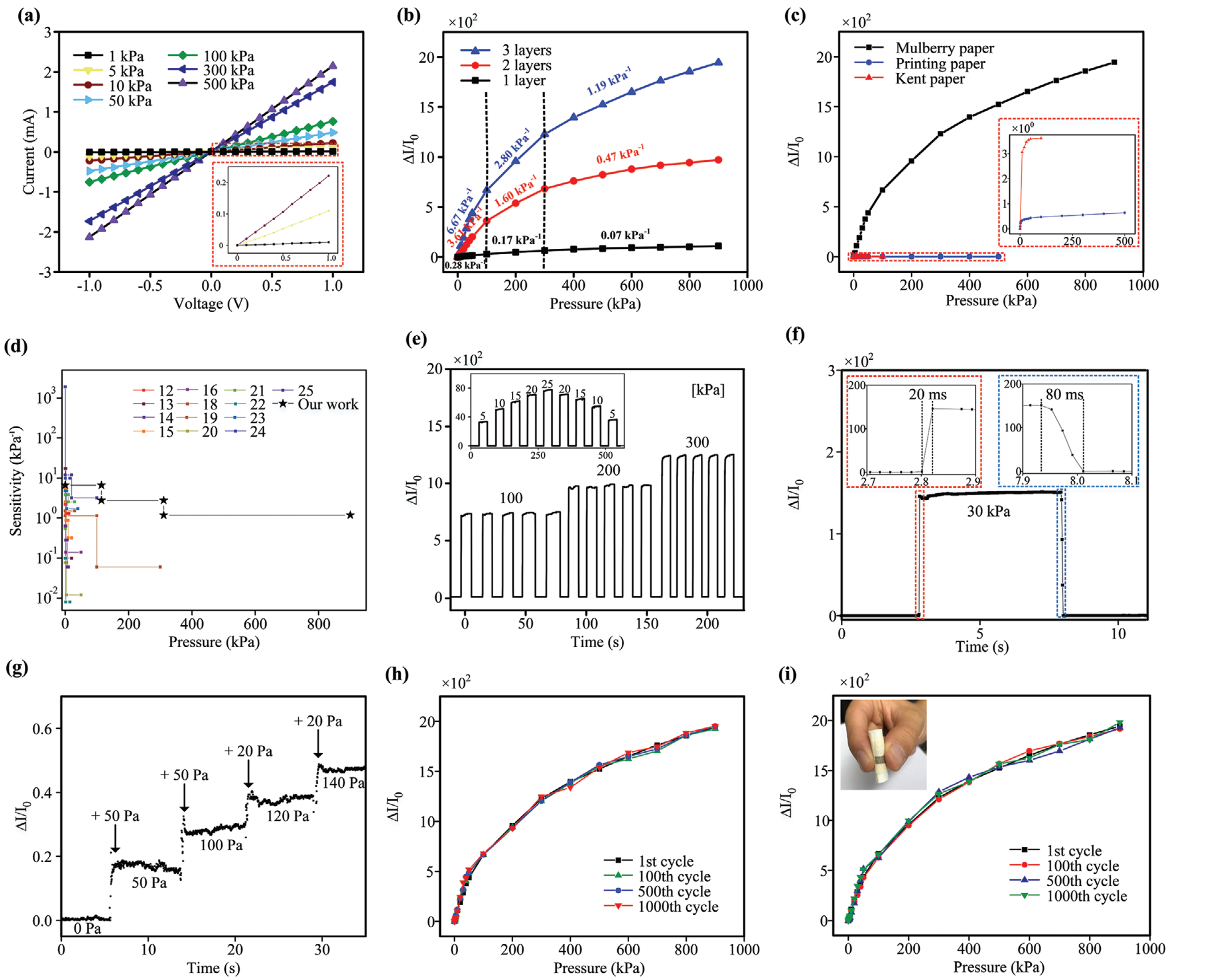


**Figure 2.** Overall pressure-sensing characteristics of sensor. a) Current–voltage curves of tactile sensor with three CNT-printed mulberry paper structures under various pressures from 1 to 500 kPa. b) Relative change in current of sensors based on one-, two-, and three mulberry paper-layered structure upon applied pressures from 1 to 900 kPa. c) Performance comparison of sensors based on mulberry paper, copy paper, and Kent paper. d) Comparison of pressure-sensing performances with respect to sensitivity and sensing range among reported paper-based tactile sensors. e) Dynamic response of sensor over time at repeated pressures of 100, 200, and 300 kPa. f) Response and relaxation time (20/80 ms) of sensor when applied pressure was 30 kPa. g) Limit of pressure detection and resolution (50/20 Pa) of sensor. h) Durability of sensor evaluated at 1000-cycled pressures from 1 to 900 kPa. i) Mechanical robustness and stability of sensor investigated via pressure-sensing characteristics after rolling it for 1000 cycles.

other papers based on the roughness felt by one's hands. In addition, mulberry paper has a highly porous networked fiber structure. The SEM images of the mulberry and copy paper are presented in Figure S7 in the Supporting Information. As shown, the structure and fiber of mulberry paper are more porous and thicker than those of copy paper. The high roughness and porosity of mulberry paper allow for relatively easy deformation, resulting in more changes in the contact area between layers under applied pressures, i.e., high sensitivity. The thicker and longer fibers of mulberry paper[30] provide structural robustness, thereby enabling pressure detection over a wide range with linearity. Figure 2d shows a comparison of the pressure-sensing performances with respect to the sensitivity and sensing range between reported paper-based tactile sensors (see Table S1 in the Supporting Information for detailed values).[12–25] Some of the reported paper-based tactile sensors indicated a high sensitivity exceeding 10 kPa$^{-1}$; however, the sensitivities were limited to narrow ranges of applied pressure, i.e., below 0.5,[24] 2,[13] and 20 kPa.[25] This is the first study to report a sensitivity exceeding 1 kPa$^{-1}$ at a wide range of pressures from 0.05 to 900 kPa among paper-based tactile sensors. This highlights that the use of mulberry paper as a structural material and the stacking strategy of CNT-printed layers is crucial for achieving high sensitivity to pressures over a wide sensing range. Figure 2e shows the dynamic response of the sensor over time at repeated pressures of 100, 200, and 300 kPa. The magnitude of $\Delta I/I_0$ at the same pressure showed no significant difference, and it clearly increased with pressure. We further investigated the response and relaxation time of the sensor, which are important for real-time applications (Figure 2f). When the applied pressure was 30 kPa, the measured response and relaxation times were 20 and 80 ms, respectively. These tens of milliseconds of response and relaxation times are comparable to those of previously reported paper-based tactile sensors.[12,15,19,21,24] We have also measured a response time for a smaller applied pressure of 5 kPa, and this additional result is presented in Figure S8 in the Supporting Information of the revised manuscript. Although this response time is somewhat longer than that for the larger pressure (30 kPa) applied, this range of response is hundreds of milliseconds comparable to those of previously reported paper-based tactile sensors.[14,16,20] In addition, we also measured the response time when the applied pressure was 50 Pa (Figure 2g), which was ≈200 ms. Additionally, the limits of pressure detection and resolution were investigated (Figure 2g); it was discovered that they were as low as 50 and 20 Pa, respectively. These low limits of pressure detection and resolution can be attributed to the hierarchical structure of fibers in the CNT-printed mulberry paper. The increase in current even at tens of Pascals of pressure implies that a new contact area was formed between the coated CNTs on the fibers of each mulberry paper. The durability of the sensor was evaluated at 1000-cycled cycles from 1 to 900 kPa (Figure 2h). No changes in $\Delta I/I_0$ were observed after 1000-cycled pressure cycles. Additionally, SEM images were obtained after pressure loading from 0 to 900 kPa for 1000 cycles to investigate the interfacial stability between the CNT- and AgNP-printed mulberry paper. Figure S9 in the Supporting Information presents the SEM image of the AgNP-printed mulberry paper in the sensor after 1000 cycles of loading. Please note that we observed the topmost fibers of AgNP-printed mulberry paper, where CNTs were most likely transferred from the CNT-printed paper. We confirmed that only a few CNTs were transferred to the AgNP-printed mulberry paper even after repeated loading for 1000 cycles. Meanwhile, the sensor performance showed no significant change after 1000 cycles, as shown in Figure 2h. If the interfacial stability between CNTs and AgNPs or CNTs and CNTs was poor, the sensor performance would have degraded significantly. Hence, we expect that the presented sensor can be utilized for long-time or long-term operation without interfacial instability issues between layers. The mechanical robustness and stability of the sensor were investigated based on its pressure-sensing characteristics after it was rolled for 1000 cycles (Figure 2i). No significant changes in $\Delta I/I_0$ were observed, even after 1000 cycles of rolling. The high durability and mechanical stability were attributed to the robustness of mulberry paper, as discussed above. We performed experiments to confirm the durability and stability of the sensor after folding and crumpling. The results are presented in Figure S10 in the Supporting Information, and the experimental conditions are shown in the inset. We observed a small decrease in sensitivity after folding the sensor, which was maintained to some extent after 1000 cycles. However, under harsher conditions, such as crumpling the sensor for 1000 cycles, the sensitivity decreases by approximately half of the initial value. A tear in the mulberry paper or a separation between the layered structures was observed after crumpling for 1000 cycles, which would induce a decrease in the sensitivity of the sensor. Nevertheless, we believe the result is still meaningful because this is the first study, to the best of our knowledge, to present the sensing performance of the paper-based tactile sensors after crumpling for many cycles. Furthermore, we compared the pressure-sensing performances of different sensors prepared using the same method to confirm the reproducibility of our approach (Figure S11, Supporting Information). Although a slight difference in pressure-sensing characteristics was observed among the three sensors, a wide sensing range with high sensitivity was achieved in all of them, indicating the significant advantage of our approach of using mulberry paper in a paper-based tactile sensor. Another point to be considered is the interaction or bonding force between the mulberry paper bonded with an adhesive. To evaluate the interaction/bonding force between mulberry paper, a T-peel test was performed, as shown in Figure S12 in the Supporting Information.[38] A specimen comprised of two mulberry papers bonded with a glue stick was prepared with a width of 2 cm and a length of 10 cm. The average peel strength (≈5.51 N m$^{-1}$) was calculated as the peel force over the elongation length (red line in Figure S12 in the Supporting Information). However, with this peel strength, firm bonding was not maintained after the sensor was crumpled for 1000 cycles, although we could not observe the separation of mulberry paper after identical cycles of rolling or folding tests. The bonding force between mulberry paper is not sufficient to endure harsh conditions such as many times of crumpling, and the enhanced adhesion strategy will be presented in future work.

### 2.3. Various Applications

Recognizing that multipoint pressures is necessary for advanced technologies using tactile sensors, such as remote surgery and human–machine interfaces, an array using multiple tactile sensing elements with row and column electrodes was introduced. However, electrical crosstalk originating from the leakage current between the adjacent cells of a pressure sensor array is an issue that needs to be addressed.[39,40] To prevent this undesirable crosstalk effect, various techniques have been developed, such as using an active matrix or implementing a structural change.[41,42] However, these methods require complex circuits or manufacturing processes. Herein, we present a pressure sensor array based on mulberry paper prepared by simple and cost-effective inkjet printing. A schematic illustration of the constructed 3 × 3 array is shown in **Figure 3**a. Each cell of the array had a footprint area of 1 cm$^2$, and the spacing between them was 0.3 cm. Inkjet printing enabled complete electrical separation between the cells, as revealed by the SEM image in Figure 1d. In other words, inkjet-printed pressure-sensing elements were electrically isolated because the dielectric area of mulberry paper existed between them. Therefore, crosstalk can be eliminated in our array. Figure 3b shows the response of the array at a pressure of 100 kPa at one point. No significant changes were observed in other cells, except for the cells applied with pressure. Each cell of the fabricated sensor array recognized the applied pressure without crosstalk with neighboring cells, as shown in Figure 3c. The current of each cell in the array was individually measured from each pair of

 

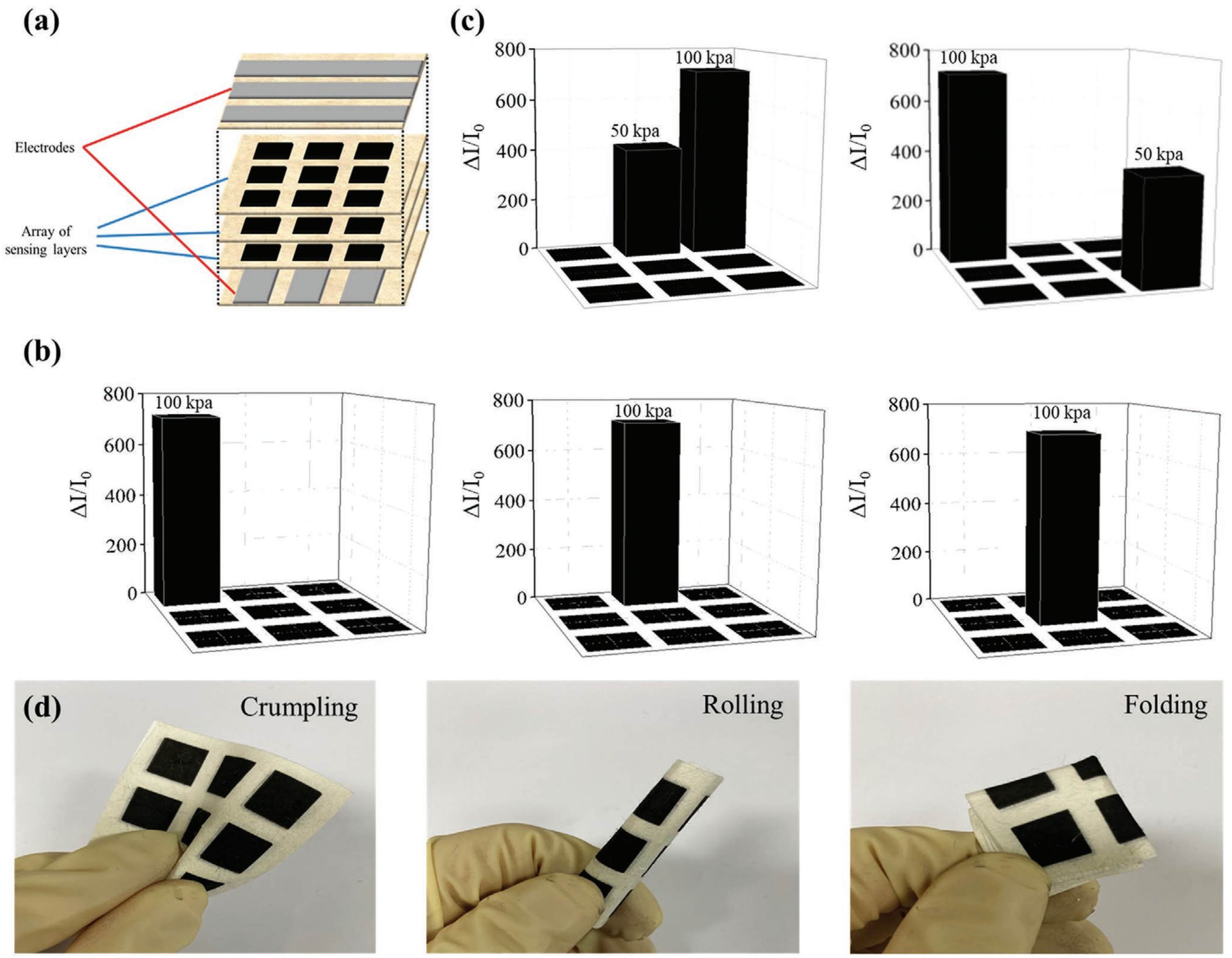


**Figure 3.** a) Schematic illustration of pressure sensor array based on mulberry paper prepared via simple and cost-effective inkjet printing (3 × 3 array). Every cell of array had a footprint area of 1 $cm^2$, and the spacing between them was 0.3 cm. b) Response of array with a pressure of 100 kPa at one point. No significant changes observed in other cells except the cell applied with pressure. c) Recognition of independent pressures without crosstalk. d) Photographs of mulberry paper-based tactile sensor array when it was crumpled, rolled, and folded. Results show high flexibility of sensor comprising multilayer mulberry paper.

electrodes while maintaining the pressure applied to specific or multiple locations. For example, when the pressure at two points was simultaneously applied with weights of 0.5 and 1 kg, which corresponded to 50 and 100 kPa, respectively, the current through nine individual cells in the array was sequently measured using a sourcemeter without a significant time lag. Although the distance between the cells was quite long (0.3 cm), the spatial resolution can be enhanced because inkjet printing can offer a resolution of tens of microns.[43] Hence, we are further studying the relation of how high spatial resolution can be achieved without mechanical crosstalk induced by the structural change of adjacent cells. Figure 3d shows photographs used to investigate the mechanical robustness of the mulberry paper-based tactile sensor array when it was crumpled, rolled, and folded. The results showed the high flexibility of the sensor array, which comprised multilayer mulberry paper.

Multiaxis pressure detection with flexibility is a key requirement for a robotic finger that mimics human perception to prevent poorly directed or excessive grip force.[44] Hence, based on the high flexibility of mulberry paper, we demonstrated a three-axis pressure sensor capable of measuring normal and shear forces. The three-axis pressure sensor comprised four cells that can detect shear force,[45] as shown in **Figure 4**a, and the z-direction force was calculated as the sum of the four cells. In addition, the design of the sensor can be easily changed using inkjet printing to achieve the desired purpose. A hemispherical controller (Figure 4a) was designed and fabricated via 3D printing and was subsequently attached to a sensor with three CNT-printed layers between two AgNP-printed electrodes (see Figure S13 in the Supporting Information for details regarding the structure and detailed sensing mechanism of the three-axis pressure sensor). A microcontroller unit (Arduino Uno) was used to measure the sensor signal and convert it into a vector that indicates the direction and magnitude of the force. Subsequently, the converted vectors were visualized in real time using MATLAB (Figure 4b,c). As shown in Movie S1

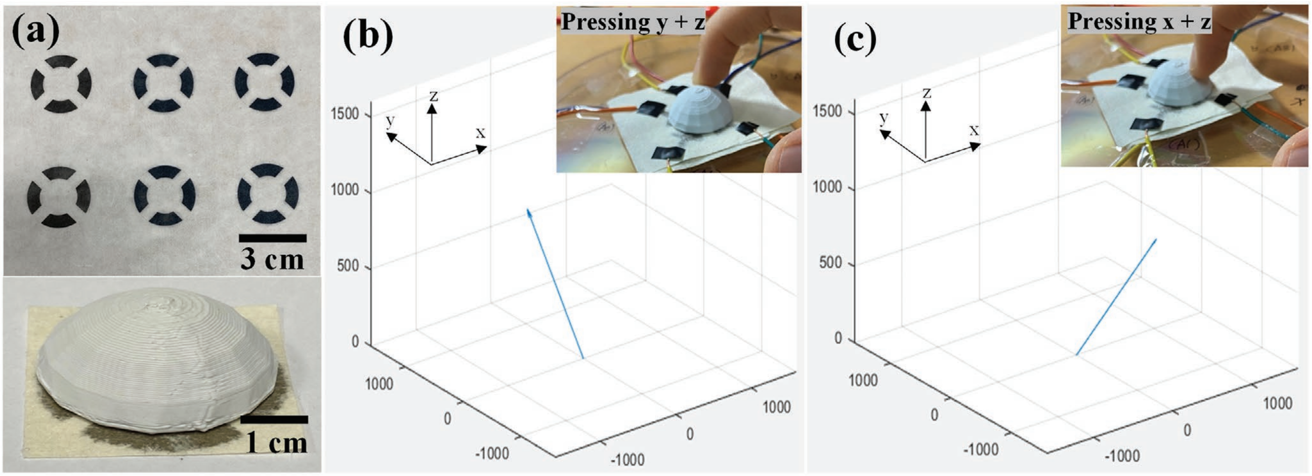


**Figure 4.** a) Three-axis pressure sensor composed of four cells for detecting shear force. A hemispherical controller was designed and fabricated via 3D printing and then attached to a sensor having three CNT-printed mulberry paper layers between two Ag NP-printed electrodes. b,c) Pressure vectors converted and visualized in real time using a microcontroller unit and MATLAB, respectively. Fabricated three-axis pressure sensor shows highly sensitive and fast response in real time upon applied pressures, with no significant time lag.

in the Supporting Information, the three-axis pressure sensor indicates a highly sensitive and fast response in real-time under applied pressures with no significant time lag. This is attributed to the inherent characteristics of our approach using mulberry paper as the constructional material of the sensor, as discussed in the previous section.

Mulberry paper is thin, lightweight, biocompatible, foldable/bendable, and highly stable to chemicals. To utilize these characteristics, we fabricated a tactile sensor as a wearable device. The sensor was placed on the neck of a human body using an exercise band, and a pulse was detected through the sensor as a wearable device with high sensitivity. **Figure 5**a shows the real-time response of the sensor; the measured periodicity of the artery pulse was shown to be ≈72 beats $min^{-1}$, confirming that it was the pulse of an ordinary 29-year-old man. The enlarged pulse signal at the neck of the subject is shown in Figure 5b. This shows the distinctive pulse peaks originating from the superposition of percussion, tidal, and diastolic blood waves.[46,47] Meanwhile, the data presented in Figure 5a,b would not reveal the sharp wave peaks. This may be because of measurement noise or short response/relaxation times at low pressure (≈200 ms). Nonetheless, we believe that it is still meaningful in that we presented the potential applications of our mulberry paper-based tactile sensor. To demonstrate another wearable device application that requires a wide pressure-sensing range of the sensor, we attached the sensor to the shoe of a user to detect his/her movements. When the user walks or runs, the sensor measures the pressure applied to the shoe in real time. Figure 5c shows the response of the sensor attached to the shoe when the user walked, ran, and walked again. The inset of Figure 5c presents a photograph of the sensor attached to the shoe. Higher responses and frequencies were observed when the user was running compared to the response when the user was walking. These results indicate that our sensor can detect foot pressures up to several hundred kilopascals[35] and distinguish the frequency in real time. Furthermore, we demonstrated exercise monitoring using the fabricated tactile sensor. As a proof of concept, the user performed a squat thrust while wearing the sensor-attached shoe (Figure 5d). The speed, number, count, and balance of the squats were measured when the exercise was performed. If the user loses balance during the exercise, the sensor signal drifts significantly; however, the magnitude and frequency of the measured responses are stable. Hence, our approach of using a mulberry paper-based tactile sensor is suitable even for exercise monitoring based on foot pressure distribution, as it can be further advanced using an array with the enhanced spatial resolution of inkjet printing.

## 3. Conclusion

We demonstrated all paper-based tactile sensors using CNT-printed mulberry paper with a multilayer structure as a pressure-sensing element and AgNP-printed mulberry paper as electrodes. Inkjet printing enabled a conformal CNT coating on the fibers of the mulberry paper, which was advantageous for tactile sensors based on changes in contact resistance. We utilized the noble characteristics of mulberry paper, such as its rough surface and highly porous fiber-networked structure, which induced a significant change in the contact area of the trilayer stacked structure, resulting in high sensitivity over a wide pressure range (6.67 $kPa^{-1}$ at 0.05–100 kPa, 2.80$kPa^{-1}$ at 100–300 kPa, and 1.19 $kPa^{-1}$ at 300–900 kPa). The enhanced mechanical robustness of mulberry paper provided a wide pressure-sensing range compared with those of printing and Kent paper. Notably, this is the first study among paper-based tactile sensors that report both a wide sensing range from 0.05 to 900 kPa and a high sensitivity of over 1 $kPa^{-1}$. In addition, the fabricated sensor demonstrated a fast response and relaxation time (20/80 ms), as well as a low limit of detection (50 Pa) and a high resolution (20 Pa). The excellent durability and flexibility of the sensor were validated through repeated application of pressures and even rolling. Because of the outstanding performance of the sensor, we applied it to various applications, including a crosstalk-free

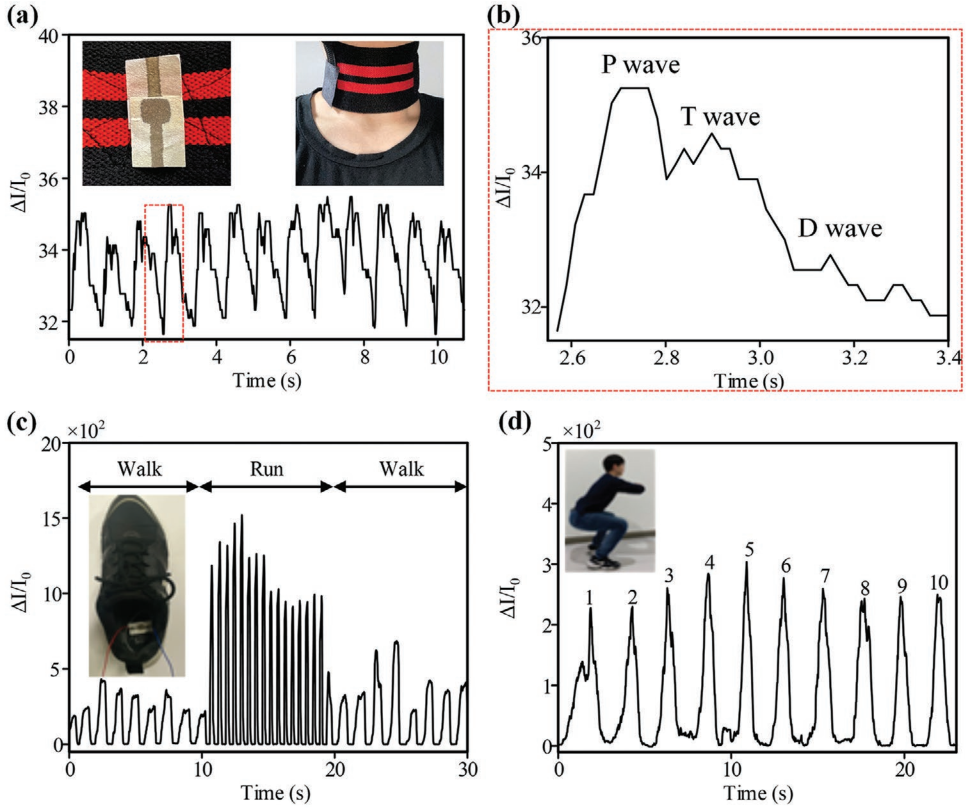


**Figure 5.** a) Real-time response of sensor at the neck of a subject, revealing that the measured periodicity of artery pulse (72 beats $\min^{-1}$). b) Enlarged pulse signal at the neck of subject; distinctive pulse peaks originating from the superposition of percussion, tidal, and diastolic blood waves are clearly shown. c) Response of sensor attached to shoe when user walks, runs, and walks again, successively. d) Exercise monitoring using fabricated tactile sensor. User performs squat thrust while wearing sensor-attached shoe.

pressure sensor array, a three-axis pressure sensor, and wearable devices for monitoring physiological signals from a user. The high sensitivity, high flexibility, wide sensing range, low cost, mass-producible fabrication method, and high durability of our sensor render it a promising solution for paper-based tactile sensors.

## 4. Experimental Section

*Fabrication of Mulberry Paper-Based Tactile Sensor*: The sensor was fabricated using commercially available mulberry paper (Samwon, Inc.) as a structural material. Deionized water-based 2 wt% multiwalled carbon nanotube (MWCNT) (diameter: 20 nm, length ≈10 µm) ink purchased from Applied Carbon Nano Inc. was used as the printing material for the pressure-sensing layer. The electrode was prepared by printing a triethylene glycol monomethyl ether-based 30 wt% AgNP ink purchased from Sigma–Aldrich. Before printing was performed with an inkjet printer, the ink inside the cartridge was replaced with CNTs and AgNP ink. A perforation was created in the upper part of the cartridge, and the originally filled ink was removed via suction using a syringe. Subsequently, the emptied cartridge was filled with CNT ink and AgNP ink using a syringe. The electrode and sensing layer were printed using an inkjet printer (OfficeJet 4655, HP). The designed area of the sensing layer was a 1 cm × 1 cm square, and that of the electrode was a 0.3 cm × 2 cm rectangle attached to a 1 cm × 1 cm square. After printing, the CNT-printed mulberry paper was dried in a convection oven at 80 °C for 10 min, and the AgNP-printed mulberry paper was sintered in an oven at 200 °C for 20 min. The CNT- and AgNP-printed mulberry paper were cut into rectangles measuring 3 cm × 4 cm and pasted using a solid adhesive (GSW10, Amos). The pressure sensor array was prepared using the same fabrication process, except for the initial design prepared using an inkjet printer.

*Characterization of Mulberry Paper-Based Tactile Sensor*: The surfaces of the copy paper, mulberry paper, and CNT-coated mulberry paper were observed via SEM (IT500HR, JEOL). To investigate the pressure sensing performance, the sensor was attached to a motorized push-pull test stand (KMX-E1000N, MAS). The amount of pressure applied to the sensor was adjusted using a motorized push-pull test stand, and a force gauge (DTG-10, Digitech) was used to measure the magnitude of the pressure. The current flowing through the sensor was measured in real time using a sourcemeter (2614 B, Keithley). The voltage applied by the sourcemeter to measure the current was 1 V.

*Three-Axis Pressure Detection and Wearable Devices with a Mulberry Paper-Based Tactile Sensor*: The electrode and sensing layers of the three-axis force sensor were prepared using the same method as that used for the mulberry paper-based tactile sensor. The sensor controller was fabricated using a 3D printer (3Dwox dp201, Sindoricoh). To measure the resistance change of each cell in the three-axis force sensor, an Arduino UNO was used to provide the voltage and read the resistance of each cell. The measured resistance was calibrated to pressures, which were subsequently plotted in MATLAB in real time. To measure the arterial pulse, the sensor was attached to the exercise band, and the band was conformally attached around the neck. To measure the foot pressure during exercise, the sensor was attached to the shoe, and the change in current resulting from the pressure change was acquired and recorded using a sourcemeter (2614 B, Keithley). Informed consent was obtained from participants who volunteered to perform these studies. All testing reported conformed to the ethical requirements of the Yonsei University.

## Supporting Information

Supporting Information is available from the Wiley Online Library or from the author.

## Acknowledgements

T.L. and Y.K. contributed equally to this work. This work was supported by the National Research Foundation of Korea (NRF) grant funded by the Korea government (MSIT) (No. 2021R1A2B5B03002850), and this work was also supported by the Korea Medical Device Development Fund grant funded by the Korea government (the Ministry of Science and ICT) (Project Number: KMDF_PR_20200901_0154).

## Conflict of Interest

The authors declare no conflict of interest.

## Data Availability Statement

Research data are not shared.

## Keywords

inkjet printing, mulberry paper, pressure sensor, paper-based tactile sensors, wide pressure range

Received: April 11, 2021
Revised: June 25, 2021
Published online:

[1] Y. Lin, D. Gritsenko, Q. Liu, X. Lu, J. Xu, *ACS Appl. Mater. Interfaces* **2016**, *8*, 20501.
[2] D.-W. Wang, F. Li, J. Zhao, W. Ren, Z.-G. Chen, J. Tan, Z.-S. Wu, I. Gentle, G. Q. Lu, H.-M. Cheng, *ACS Nano* **2009**, *3*, 1745.
[3] X. Huang, B. Sun, K. Li, S. Chen, G. Wang, *J. Mater. Chem. A* **2013**, *1*, 13484.
[4] H. Liu, G. Zhao, M. Wu, Z. Liu, D. Xiang, C. Wu, Y. Cheng, H. Wang, Z. L. Wang, L. Li, *Nano Energy* **2019**, *66*, 104161.
[5] Y. Zhang, L. Ge, M. Li, M. Yan, S. Ge, J. Yu, X. Song, B. Cao, *Chem. Commun.* **2014**, *50*, 1417.
[6] Y. Fujisaki, H. Koga, Y. Nakajima, M. Nakata, H. Tsuji, T. Yamamoto, T. Kurita, M. Nogi, N. Shimidzu, *Adv. Funct. Mater.* **2014**, *24*, 1657.
[7] W. S. Lee, J. Choi, *ACS Appl. Mater. Interfaces* **2019**, *11*, 19363.
[8] X. Zhao, W. Han, C. Zhao, S. Wang, F. Kong, X. Ji, Z. Li, X. Shen, *ACS Appl. Mater. Interfaces* **2019**, *11*, 10301.
[9] S. Cinti, L. Fiore, R. Massoud, C. Cortese, D. Moscone, G. Palleschi, F. Arduini, *Talanta* **2018**, *179*, 186.
[10] H.-P. Cong, X.-C. Ren, P. Wang, S.-H. Yu, *Energy Environ. Sci.* **2013**, *6*, 1185.
[11] D. D. Liana, B. Raguse, J. J. Gooding, E. Chow, *Adv. Mater. Technol.* **2016**, *1*, 1600143.
[12] Z. Zhan, R. Lin, V.-T. Tran, J. An, Y. Wei, H. Du, T. Tran, W. Lu, *ACS Appl. Mater. Interfaces* **2017**, *9*, 37921.
[13] L.-Q. Tao, K.-N. Zhang, H. Tian, Y. Liu, D.-Y. Wang, Y.-Q. Chen, Y. Yang, T.-L. Ren, *ACS Nano* **2017**, *11*, 8790.
[14] K. Lee, J. Lee, G. Kim, Y. Kim, S. Kang, S. Cho, S. Kim, J.-K. Kim, W. Lee, D.-E. Kim, S. Kang, D. Kim, T. Lee, W. Shim, *Small* **2017**, *13*, 1700368.
[15] S. Chen, Y. Song, F. Xu, *ACS Appl. Mater. Interfaces* **2018**, *10*, 34646.
[16] Y.-Q. Liu, Y.-L. Zhang, Z.-Z. Jiao, D.-D. Han, H.-B. Sun, *Nanoscale* **2018**, *10*, 17002.
[17] J. Fastier-Wooller, T. Dinh, V. T. Dau, H.-P. Phan, F. Yang, D. V. Dao, *Sensors* **2018**, *18*, 3300.
[18] L. Gao, C. Zhu, L. Li, C. Zhang, J. Liu, H.-D. Yu, W. Huang, *ACS Appl. Mater. Interfaces* **2019**, *11*, 25034.
[19] T. Yang, J. M. Mativetsky, *ACS Appl. Mater. Interfaces* **2019**, *11*, 26339.
[20] Z. Yu, Y. Tang, G. Cai, R. Ren, D. Tang, *Anal. Chem.* **2019**, *91*, 1222.
[21] Y. Guo, M. Zhong, Z. Fang, P. Wan, G. Yu, *Nano Lett.* **2019**, *19*, 1143.
[22] W. Li, L. Xiong, Y. Pu, Y. Quan, S. Li, *Nanoscale Res. Lett.* **2019**, *14*, 183.
[23] P. Zhao, R. Zhang, Y. Tong, X. Zhao, Q. Tang, Y. Liu, *Adv. Electron. Mater.* **2020**, *6*, 1901426.
[24] L. Gao, J. Yu, Y. Li, P. Wang, J. Shu, X. Deng, L. Li, *Nanomaterials* **2020**, *10*, 2536.
[25] P. M. Pataniya, C. K. Sumesh, M. Tannarana, C. K. Zankat, G. K. Solanki, K. D. Patel, V. M. Pathak, *Nanotechnology* **2020**, *31*, 435503.
[26] X. Lin, S. Gao, T. Fei, S. Liu, H. Zhao, T. Zhang, *Sens. Actuators, A* **2019**, *292*, 66.
[27] Y. Seo, B. Hwang, *Cellulose* **2019**, *26*, 8867.
[28] K. Wang, J. Jiang, J. Xu, J. Feng, J. Wang, *RSC Adv.* **2016**, *6*, 14164.
[29] N. Ayrilmis, A. Kaymakci, F. Ozdemir, *J. Ind. Eng. Chem.* **2013**, *19*, 908.
[30] T. G. Yun, D. Kim, S.-M. Kim, I.-D. Kim, S. Hyun, S. M. Han, *Adv. Energy Mater.* **2018**, *8*, 1800064.
[31] K. E. Lee, E. A. Sanders, in *Green Fashion* (Eds: S. S. Muthu, M. A. Gardetti), Vol 1, Springer Singapore, Singapore **2016**, p. 159.
[32] M. Go, B. Hwang, S. Lim, *Mater. Manuf. Processes* **2019**, *34*, 1605.
[33] H. Song, S. Lim, *Mater. Manuf. Processes* **2020**, *35*, 1701.
[34] X. Qi, X. Li, H. Jo, K. Sideeq Bhat, S. Kim, J. An, J.-W. Kang, S. Lim, *Sens. Actuators, A* **2020**, *301*, 111697.
[35] Y. Lee, J. Park, S. Cho, Y.-E. Shin, H. Lee, J. Kim, J. Myoung, S. Cho, S. Kang, C. Baig, H. Ko, *ACS Nano* **2018**, *12*, 4045.
[36] S. Pyo, J. Lee, W. Kim, E. Jo, J. Kim, *Adv. Funct. Mater.* **2019**, *29*, 1902484.
[37] J. Jung, G. M. Raghavendra, D. Kim, J. Seo, *Int. J. Biol. Macromol.* **2016**, *93*, 933.
[38] J. C. Yeo, J. Yu, M. Shang, K. P. Loh, C. T. Lim, *Small* **2016**, *12*, 1593.
[39] R. S. Karmakar, Y.-J. Lu, Y. Fu, K.-C. Wei, S.-H. Chan, M.-C. Wu, J.-W. Lee, T.-K. Lin, J.-C. Wang, *Sci. Rep.* **2017**, *7*, 12252.
[40] X. Wu, Y. Han, X. Zhang, Z. Zhou, C. Lu, *Adv. Funct. Mater.* **2016**, *26*, 6246.
[41] L. Nela, J. Tang, Q. Cao, G. Tulevski, S.-J. Han, *Nano Lett.* **2018**, *18*, 2054.
[42] S. Pyo, J. Choi, J. Kim, *Adv. Electron. Mater.* **2018**, *4*, 1700427.
[43] T. H. da Costa, J.-W. Choi, *Micro and Nano Syst. Lett.* **2020**, *8*, 2.
[44] T. Zhang, L. Jiang, X. Wu, W. Feng, D. Zhou, H. Liu, *IEEE/ASME Trans. Mechatron.* **2015**, *20*, 1875.
[45] S. Pyo, J.-I. Lee, M.-O. Kim, T. Chung, Y. Oh, S.-C. Lim, J. Park, J. Kim, *J. Micromech. Microeng.* **2014**, *24*, 075012.
[46] J. Lee, S. Pyo, D.-S. Kwon, E. Jo, W. Kim, J. Kim, *Small* **2019**, *15*, 1805120.
[47] Z. Wang, Y. Si, C. Zhao, D. Yu, W. Wang, G. Sun, *ACS Appl. Mater. Interfaces* **2019**, *11*, 27200.